Scaling of Misorientation Angle Distributions

D. A. Hughes,[1] D. C. Chrzan,[2,3] Q. Liu,[4] and N. Hansen[4]
[1]*Center for Materials and Applied Mechanics, Sandia National Laboratories, Livermore, California 94550*
[2]*Department of Materials Science and Mineral Engineering, University of California, Berkeley, California 94720*
[3]*Materials Sciences Division, Lawrence Berkeley Laboratory, Berkeley, California 94720*
[4]*Materials Department, Risø National Laboratory, DK 4000, Roskilde, Denmark*
(Received 26 May 1998)

The measurement of misorientation angle distributions following different amounts of deformation in cold-rolled aluminum and nickel and compressed stainless steel is reported. The scaling of the dislocation cell boundary misorientation angle distributions is studied. Surprisingly, the distributions for the small to large strain regimes for aluminum, 304L stainless steel, nickel, and copper (taken from the literature) appear to be identical. Hence the distributions may be "universal." These results have significant implications for the development of dislocation based deformation models. [S0031-9007(98)07728-X]

PACS numbers: 62.20.Fe, 61.72.Ff

Plastic deformation of metals is of great technological importance. Accordingly, a large effort has been directed towards understanding the fundamental processes leading to plastic deformation and the significant material property changes that occur. Ideally, this fundamental knowledge can be used to construct predictive, quantitative theories of plastic flow. Towards this end, identification of microstructural relationships which are invariant and/or scale during straining is important.

In most circumstances, plastic deformation is associated with the motion and subsequent trapping of dislocations within the metal. This trapping induces strength changes that depend on the number and mobility of the dislocations. Commonly during straining, dislocations organize themselves into mosaic patterns in response to both their own self stresses and the applied stress. The "mosaic," clearly visible in Fig. 1, is composed of dislocations that are arranged in nearly two dimensional boundaries surrounding regions that are almost dislocation free. The regions of crystal on either side of a dislocation boundary are slightly rotated with respect to one another, with the rotation depending on the dislocation content of the boundary. The resulting minimum angle of rotation necessary to realign the regions, the so-called boundary misorientation angle, is defined to be θ. The mosaic, or microstructural pattern, evolves with increasing stress and strain.

Empirically, the strength of a metal scales with the square root of the dislocation density and also scales inversely with the average spacing between dislocation boundaries [1,2]. Nevertheless, a comprehensive theory for the evolution of these structures with increasing strain remains elusive. (See [1,3–6] for a range of views.)

This lack of a comprehensive theory stems from a combination of factors. There is an enormous change in dislocation density during many deformation processes, e.g., from 10^{10}–10^{12} m^{-2} in the annealed state to roughly 5×10^{16} m^{-2} in the highly deformed state. Over the same strain range, the strength of the material changes by 2 orders of magnitude. The accumulating dislocations have a variety of Burgers vectors and interact through long-ranged elastic forces and short-ranged contact forces. Current theories simply cannot solve this dynamic "many-body" problem. The number of dislocations encountered in a typical deformation process is far beyond that which can be modeled using atomic scale calculations [7–10], or with current three dimensional dislocation dynamics simulations [11–14].

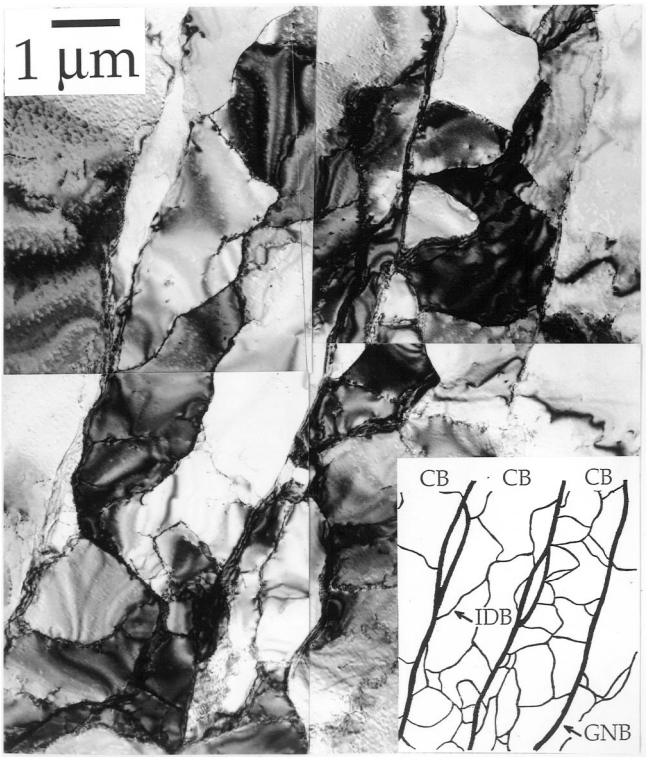

FIG. 1. TEM micrograph of pure aluminum following compression to $\varepsilon = 0.6$ showing an example of the CB dislocation structure. The CB, GNBs, and IDBs are labeled in the inset.

 0031-9007/98/81(21)/4664(4)$15.00

Thus, it is reasonable to search for parameters that characterize the evolving microstructure. The parameters used historically include the spacing between dislocation boundaries, the dislocation density, and the link length, i.e., length of dislocation line between nodes in a dislocation boundary. Measurement of link length distributions following high temperature creep led to early scaling analyses related to plastic deformation. In these analyses, the shape of the link length distribution, when appropriately scaled using the average link length, remains invariant during creep. Bilde-Sorenson observed scaling of dislocation link length distributions in high temperature creep deformed MgO [15]. Later, Lin *et al.* [16] observed scaling of the dislocation link length distributions in NaCl and Al deformed under creep conditions.

Here, it is demonstrated that a similar invariant form exists for general monotonic deformation modes: the misorientation angle distribution, i.e., the θ distribution. Recently, the present authors reported that the evolution of the θ distribution associated with one type of dislocation boundary, incidental dislocation boundaries (IDBs) in cold-rolled high purity Al, is consistent with a scaling hypothesis [17]. In this scaling analysis, the scaling parameter is the average misorientation angle, θ_{av} which increases as a function of increasing strain.

To explore the nature of the observed scaling, a new series of measurements was conducted. This series was chosen to investigate key factors that make large differences in the motion of individual dislocations and in macroscopic mechanical properties. The investigated factors include stacking fault energy (SFE), the presence of solute atoms, temperature, strain rate, monotonic deformation mode, and amount of strain (Table I). The variation in these factors is limited to those conditions in which a dislocation may move on more than one slip plane or may climb perpendicular to that plane. Dislocation motion in three dimensions is known to be a necessary component of cell boundary formation [5,6]. These new experiments demonstrate that the shape of the θ distribution when scaled by θ_{av} is insensitive to many factors thought to govern dislocation dynamics, microstructure evolution, and mechanical properties.

This result is surprising for many reasons. For example: (i) SFE influences the dislocation core configuration and thereby the dislocation's ability to glide onto an intersecting slip plane. Three-dimensional mobility increases with increasing SFE [18] from very low mobility in 304L stainless steel to very high mobility in aluminum (see Table I). As a result, dislocation cell structures are not formed during room temperature deformation of stainless steel. However, cells are formed at higher temperatures. (ii) Solute atoms, such as those in stainless steel and commercial purity aluminum, interact strongly with gliding dislocations so that even small concentrations of solute atoms have large effects on strength [18]. Solute atoms may also affect the nucleation of dislocation boundaries through this interaction. (iii) Temperature and strain rate change the average velocity of thermally activated glide of dislocations past obstacles and also the rate of dislocation climb processes. Dislocation climb will provide additional short range three dimensional mobility of dislocations for deformation temperatures above one half of the melting temperature T_m. (iv) Deformation mode determines slip system activity and hence the Burgers vector population of dislocations. Different slip systems are required to make the macroscopic shape change in uniaxial compression compared to that of the plane strain constraint conditions of rolling. (v) Strain changes the evolutionary stage of the microstructure. It is not expected *a priori* that the θ distributions should behave similarly irrespective of the different processes outlined above.

A typical postdeformation microstructure appears in Fig. 1. The clear mosaic pattern is composed of two types of dislocation boundaries: IDBs and those referred to as geometrically necessary boundaries (GNBs) [19,20]. This duplex structure is typically observed for monotonic deformation modes including rolling, torsion, and compression [19]. The micrograph clearly reveals the different morphologies associated with the two boundary types. GNBs are long, nearly planar boundaries that

TABLE I. Range of parameters characterizing the experiments used in construction of Fig. 2.

Material	Deformation mode	von Mises strain	Strain rate (s^{-1})	T (K)	T/T_m	SFE[a] (mJ/m^2)	θ_{av} (deg)
Al (99.996%, polycrystal)	rolling	0.06	1 to 10	293	0.31	135	0.48
		0.12	1 to 10	293	0.31	135	0.61
		0.41	1 to 10	293	0.31	135	1.02
		0.80	1 to 10	293	0.31	135	1.24
Al (99.8%, polycrystal)	rolling	2.7	1 to 10	293	0.31	135	3.0
304L stainless steel (polycrystal)[b]	compression	0.40	10^{-3}	1273	0.75	30	2.1
Cu (99.99%, single crystal)	compression	0.20	10^{-2}	873	0.64	80	2.3
Ni (99.99%, polycrystal)	rolling	4.5	1 to 10	293	0.15	160	2.9

[a]References [26–29].
[b]Nominally 18 wt% Cr, 8 wt% Ni, 2 wt% Mn, and <0.03 wt% C, with the remainder Fe.

enclose cell blocks (CBs) of several approximately equiaxed cells. The cell boundaries are IDBs.

It is hypothesized that these two boundary types form and evolve differently [19,20]. For IDBs, the underlying mechanism is thought to be the statistical trapping of glide dislocations. GNB formation is related either to differences in the slip systems operating in neighboring regions, to the operation of the same slip systems but with differing shear amplitudes, or to local strain differences. On average GNBs develop much larger values of θ_{av} than IDBs due to these different mechanisms [19,21]. For each boundary type, microstructural evolution with increasing stress and strain results in an increase in a misorientation angle that is inversely related to the decrease in spacing between the boundaries [17,22].

The distinction made between these two types of boundaries is warranted not only by the evidence of morphological differences, average misorientation angle and spacing, but also by the scaling behavior plotted in Ref. [17] and in this paper. Note the importance of first discovering this classification of boundaries as IDBs. This classification is important to the later finding of the scaling behaviors since a single grouping of the data from IDBs and GNBs does *not* yield scaling behavior [17].

Using transmission electron microscopy (TEM) the boundaries are identified, according to their morphology. Experimentally, a boundary is classified as a GNB if it extends along more than three cells lengths; the rest of the boundaries are classified as IDBs. In general, over the entire strain range investigated, GNBs are much longer than this working definition. However, as a complication at large strains, some cells increase their angle to the extent that they become equiaxed subgrains. While these subgrain boundaries are GNBs [20], they are included as part of the IDB measurement error.

TEM Kikuchi pattern analysis [23] is used to measure orientations of adjacent crystallites separated by dislocation boundaries. From these measurements, the misorientation associated with each of the boundaries is deduced. The (symmetry dictated) maximum possible θ in cubic crystals is 62.8°. Identification of the rotation axis completes the description of the misorientation. The rotation axes observed for IDBs were randomly distributed about all possible crystal axes. Hundreds of measurements are made for each strain to construct the θ distribution.

One defines formally the θ distribution, $p(\theta, \theta_{\mathrm{av}})d\theta$, as the probability that a boundary selected at random is associated with misorientation angle between θ and $\theta + d\theta$ given that the average misorientation angle is θ_{av}. (The boundaries are not weighted by their lengths.)

It was demonstrated earlier that for cold-rolled Al, $\theta_{\mathrm{av}} \sim k\varepsilon^{1/2}$ for IDBs, with ε the von Mises strain and k a constant depending on material and deformation conditions [17]. The scaling analysis, based on scaling the distributions with θ_{av} implied that the influence of ε on the θ distribution is exerted only through the parameter θ_{av}. Under these circumstances, one may cast the scaling hypothesis of Ref. [17] in a form reflecting the total strain:

$$\tilde{p}(\theta, \varepsilon) = \varepsilon^{-1/2} g(\theta/\varepsilon^{1/2}), \tag{1}$$

where $\tilde{p}(\theta, \varepsilon)$ is the misorientation angle distribution measured at a strain ε, and $g(x)$ is a scaling function defined by this equation. It is expected that $g(x)$ is material and deformation mode dependent.

Scaling the distributions using θ_{av} eliminates the material and deformation mode dependence. It is hypothesized that the θ distributions obey the following scaling form:

$$p(\theta, \theta_{\mathrm{av}}) = \theta_{\mathrm{av}}^{\beta} f\left(\frac{\theta}{\theta_{\mathrm{av}}^{\delta}}\right). \tag{2}$$

It is simple to demonstrate from the constraints on the probability distributions that $\delta = 1$ and $\beta = -1$, i.e., the average misorientation angle is θ_{av} and the integral of the distribution from $\theta = 0$ to $\theta = \infty$ is unity. (It has been assumed that the misorientation angle distribution is not yet affected by the existence of the maximum misorientation angle of 62.8°.) If this hypothesis is correct, plotting $\theta_{\mathrm{av}} p(\theta, \theta_{\mathrm{av}})$ as a function of $\frac{\theta}{\theta_{\mathrm{av}}}$ should yield one curve, *independent of* θ_{av}. The function $f(x)$ is referred to as the scaling function. (Pantleon discusses the possible origins of the shape of this function [24,25]. Pantleon's analysis is an important first step. One critical future step is to address the concurrent nucleation of new boundaries and strain evolution of existing boundaries.)

Having provided the necessary microstructural definitions, the experiments listed in Table I are used to test the generality of the scaling hypothesis, Eq. (2) . The values of θ_{av} for the IDBs are given in Table I. The measured θ distributions are used to test the hypothesis, Eq. (2). The cataloged data is binned, and a histogram is constructed as outlined in [17]. This histogram is used to construct an experimental θ distribution. The measured distributions are then plotted as described above, Fig. 2. The Cu data is taken from Ref. [24] and the low strain Al data from Ref. [17].

Within experimental error, the distributions derived from IDBs are consistent with the scaling hypothesis. The scaled distributions for Cu and for 304L stainless steel, compression tested at temperatures of 873 and 1273 K, respectively, fall on the data derived from the experiments on high and low purity Al at 293 K. Remarkably, the scaling hypothesis remains consistent for the IDB distributions following a strain of 2.7 in Al. The very high strain Ni data, while apparently scaling, has a slightly higher peak than the other data hinting at a deviation from scaling.

The implication of the above observations is that some materials properties do not affect the evolution of the θ distributions as long as a dislocation cell structure is formed. These material properties include SFE and solute content. The distribution is also invariant with respect to details of dislocation motion. Thus it appears that under

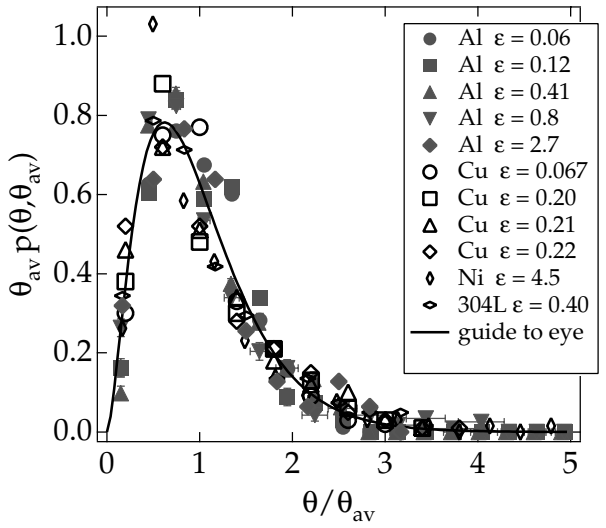

FIG. 2. Distributions scaled according to Eq. (2). Statistical error bars are shown, when available.

conditions in which cell formation occurs, cell formation does not depend on the dislocation mobility.

The observation of scaling is beneficial to one modeling the evolution of these distributions. The argument proceeds as follows. Since the time evolution of the distribution during deformation depends only on the average misorientation angle, one can devote effort to calculating the evolution of this *average* quantity. The average quantity changes with strain, material, deformation mode and temperature. The insensitivity of the distribution to material type suggests that one may be able to obtain the shape of the scaling function through analysis of simple models (see, for example, Ref. [24]). These calculations may provide a complete picture of IDB evolution.

The above observations place limitations on any theory of plastic deformation governing the regime in which cells are formed. The theory must be able to produce θ distributions which scale as observed here and must explain the apparent "universal" shape for the distribution.

In conclusion, it is argued that θ distributions provide a convenient means to characterize the microstructural evolution of these materials. Further, the experiments reported herein demonstrate that the θ distributions associated with IDBs display scaling, and the scaling function is, within experimental error, *identical* for Cu, 304L stainless steel, Al, and perhaps Ni, deformed under a wide range of conditions. Hence the θ distribution may be universal. These observations provide important constraints for predictive models for microstructural evolution.

N. Bartelt is thanked for his critical reading of this manuscript. D. A. H. and D. C. C. acknowledge the support of the Department of Energy, Office of Basic Energy Sciences, Division of Materials Sciences under Contracts No. DE-AC04-94AL85000 and No. DE-AC03-76SF00098.

[1] H. Mughrabi, in *Constitutive Equations in Plasticity*, edited by A. S. Argon (M.I.T. Press, Cambridge, MA, 1977), p. 199.
[2] S. V. Raj and G. M. Pharr, Mater. Sci. Eng. **81**, 217 (1986).
[3] U. F. Kocks, Philos. Mag. **13**, 541 (1966).
[4] F. Prinz and A. S. Argon, Phys. Status Solidi A **57**, 741 (1980).
[5] N. Hansen and D. Kuhlmann-Wilsdorf, Mater. Sci. Eng. **81**, 141 (1986).
[6] D. Kuhlmann-Wilsdorf, Mater. Sci. Eng. A **113**, 1 (1989).
[7] S. Kohlhoff, P. Gumbsch, and H. F. Fischmeister, Philos. Mag. A **64**, 851 (1991).
[8] V. Shenoy *et al.*, Phys. Rev. Lett. **80**, 742 (1998).
[9] E. Tadmor, M. Ortiz, and R. Phillips, Philos. Mag. A **73**, 1529 (1996).
[10] M. I. Baskes, C. F. Melius, and W. D. Wilson, in *Interatomic Potentials and Crystalline Defects*, edited by J. K. Lee (T.M.S., Warrendale, PA, 1980), p. 249.
[11] L. Kubin *et al.*, Solid State Phenom. **23–24**, 455 (1992).
[12] M. Rhee *et al.*, Model. Mater. Sci. Eng. **6**, 467 (1998).
[13] M. Tang, L. P. Kubin, and G. R. Canova, Acta Mater. **46**, 3221 (1998).
[14] M. C. Fivel, T. J. Gosling, and G. R. Canova, Model. Simul. Mater. Sci. Eng. **4**, 581 (1996).
[15] J. B. Bilde-Sorensen, Acta Metall. **21**, 1495 (1973).
[16] P. Lin, S. S. Lee, and A. J. Ardell, Acta Metall. **37**, 739 (1989).
[17] D. A. Hughes, Q. Liu, D. C. Chrzan, and N. Hansen, Acta Mater. **45**, 105 (1997).
[18] J. P. Hirth and J. Lothe, *Theory of Dislocations* (Krieger Publishing Company, Malabar, Florida, 1992), 2nd ed.
[19] B. Bay, N. Hansen, D. A. Hughes, and D. Kuhlmann-Wilsdorf, Acta Metall. Mater. **40**, 205 (1992).
[20] D. Kuhlmann-Wilsdorf and N. Hansen, Scr. Metall. **25**, 1557 (1991).
[21] Q. Liu and N. Hansen, Scr. Metall. Mater. **32**, 1289 (1995).
[22] N. Hansen and D. A. Hughes, Phys. Status Solidi (b) **149**, 155 (1995).
[23] Q. Liu, J. Appl. Crystallogr. **27**, 755 (1994).
[24] W. Pantleon, Scr. Mater. **35**, 511 (1996).
[25] W. Pantleon, Acta Mater. **46**, 451 (1998).
[26] B. E. P. Beeston, I. L. Dillmore, and R. E. Smallman, Met. Sci. J. **2**, 12 (1962).
[27] R. P. Reed and R. E. Schram, J. Appl. Phys. **45**, 4705 (1974).
[28] R. E. Schram and R. P. Reed, Metall. Trans. A **6**, 1345 (1975).
[29] R. E. Stoltz and J. B. Van der Sande, Metall. Trans. A **11**, 1033 (1980).